Journal of Inorganic and Organometallic Polymers and Materials (2022) 32:161–168
https://doi.org/10.1007/s10904-021-02108-9

Preparation and Adsorption Properties of Lanthanide Ion Surface-Imprinted Polymer Based on Reaming MCM-41

Yuanyuan Qin[1] · Xiu Wang[1] · Minxin Shi[1] · Yuhua Huang[1] · Xiaogang Liu[1] · Xiancai Li[1]

Received: 12 July 2021 / Accepted: 12 September 2021 / Published online: 30 October 2021

Abstract
In this paper, APTES was used as the functional monomer, reamed MCM-41 was used as the carrier, and epichlorohydrin was used as the crosslinking agent to prepare the Lanthanide ion-imprinted polymer, La-IIP. The effects of pH, time, temperature, and initial concentration on La-IIP adsorption were investigated, and the adsorption mechanism was discussed by fitting the adsorption data to various kinetic and thermodynamic models. The results showed that La-IIP reached adsorption equilibrium in 20 min at 338 K and pH = 5, and the maximum adsorption capacity was 272.2 mg/g. The La-IIP adsorption process conformed to the Langmuir adsorption model, and La-IIP showed strong selectivity for La(III) in the presence of interfering ions with similarproperties. 2 M hydrochloric acid solution was used to eluate La-IIP and re-adsorb lanthanum ion solution. After elution of La-IIP for five times, the adsorption remained at the initial value of 81%. It shows that La-IIP has stability and reusability.

Keywords Surface ion-imprinted polymer · APTES · MCM-41 · Selectivity

1 Introduction

Lanthanum is the second most-abundant rare earth metal, and most lanthanum or lanthanum-containing compounds are derived from solitary sand or extracted from mines [1]. Lanthanum is widely used in industry. High-purity lanthanum oxide is used to coat many precision instrument lenses, and lanthanum-nickel alloys are used as hydrogen storage materials [2, 3]. Lanthanum also has irreplaceable uses in the field of catalysis [4, 5]. Rare earth metals are nonrenewable resources that are being depleted due to constant exploitation and mining. Therefore, the preparation of efficient materials, and the enrichment and recovery of these rare earth elements are being investigated.

Surface ion-imprinted polymers are derivatives of ion-imprinted polymers in which the carrier is grafted with a functional monomer, and template ions are crosslinked and then eluted [6]. After removing template ions, the prepared polymer can selectively adsorb ions from solution according to its imprinted hole memory [7, 8]. Surface-imprinted polymers prevent ions from becoming too deeply embedded in the adsorbent and also contain adsorption sites on their surface. Combined, these properties improve the adsorption selectivity and speed of the polymer, which allow these materials to be used for recycling and separating rare-earth ions.

In this work, the polymer with reamed MCM-41 as the carrier was prepared. This carrier has larger adsorption capacity and pore diameter than the traditional MCM-41 [9], which is conducive to the speed of ions entering the channel, and provides a large space for the diffusion of ions or groups in the channel. The lanthanum ion surface imprinted polymer was prepared by using this advantage combined with ion imprinting technology. The experimental results showed that the imprinted polymer has large adsorption capacity for lanthanum ions and good recognition selectivity.

2 Experimental

2.1 Chemical and Reagents

$La(NO_3)_3{\cdot}6H_2O$, $Ce(NO_3)_3{\cdot}6H_2O$, $Gd(NO_3)_3{\cdot}6H_2O$, $Yb(NO_3)_3{\cdot}5H_2O$, and hexadecyltrimethyl ammonium bromide (CTAB) were obtained from Sinopharm Chemical

✉ Xiancai Li
xcli@ncu.edu.cn

[1] College of Chemistry, Nanchang University, Nanchang 330031, China

Reagent Co., Ltd. Hydrochloric acid (HCl), $Al(NO_3)_3{\cdot}9H_2O$, $Fe(NO_3)_3{\cdot}9H_2O$, and $NH_3{\cdot}H_2O$ were purchased from Xilong Scientific Co., Ltd. Tetraethyl orthosilicate (TEOS, 98%), 3-aminopropyltriethoxysilane (APTES), and 3-chloropropyltriethoxysilane were obtained from Aladdin Reagent. Arsenazo (III), and Mesitylene (MES) were obtained from Shanghai Macklin Biochemical Co., Ltd. Distilled water was used throughout the experiments. All chemical reagents and solvents were of analytical grades (AR) and used without further purification.

2.2 Preparation of Lanthanum Ion-Imprinted Polymer

2.2.1 Preparation of Reaming MCM-41

Four MCM-41 compositions were prepared using 1,3,5-trimethylbenzene (MES) as the pore expanding agent. The molar ratios of CTAB-to-1,3,5-trimethylbenzene were 1:1, 1:2, 1:3, and 1:4. First, 1.2 g CTAB, 90 mL ammonia and 130 mL deionized water were poured into a three-necked flas-k. After CTAB was fully hydrolyzed in water, CTAB were added: the molar ratio of MES was 1, 2, 3 and 4 corresponding proportions of 1,3,5-trimethylbenzene. The evenly mixed solution was stirred in water bath at 60 ℃ for 1 h, then 5 mL TEOS was slowly added, and the stirring continued for 6 h. The product was crystallized at room temperature for 3 days, and the product was recorded as MCM-41-X (X = 1, 2, 3, 4) by filtration, washing, drying and calcination. When the molar ratio of CTAB:MES was 1:2, the adsorption effect on lanthanum ions was the best, so the subsequent experiments used this ratio for reaming MCM-41. Named MCM-41-2.

2.2.2 Alkylation of MCM-41-2

MCM-41-2 prepared with a CTAB-to-mesitylene molar ratio of 1:2 was used as the carrier for alkylation. First, appropriate amounts of MCM-41-2 and xylene were mixed, stirred at 90 °C for 0.5 h. Then, 1 mL of 3-chloropropyltriethoxysilane was added, and the mixture was stirred for an additional 6 h. The mixture was suction filtered and washed repeatedly with acetone and ethanol solution, then dried at 80 °C for 8 h to obtain alkylated MCM-41-2 [10].

2.2.3 Preparation of Lanthanum Ion-Imprinted Polymer

First, 2.5 mL of APTES, 0.2339 g of anhydrous lanthanum nitrate, and 30 mL of anhydrous methanol were added to a three-necked flask, and the mixture was stirred at 50 °C for 1 h. Then, 1 g of alkylated MCM-41-2 was added, and the reaction was continued for 18 h. Anhydrous methanol was used to repeatedly wash the solid at room temperature, which was then suction filtered to remove unreacted functional monomers and lanthanum ions. The obtained product was dried at 80 °C for 8 h and then added to a flask containing 100 mL of anhydrous methanol and mixed uniformly. Then, 5 mL of epichlorohydrin was added dropwise, and then reacted at 50 °C for 12 h. The obtained product was washed with anhydrous methanol and repeatedly eluted with 2 M HCl until no lanthanum ions were present in the filtrate. Finally, it was washed with water to neutrality and dried at 80 °C for 8 h. The obtained product was denoted as La-IIP. The method for preparing non-ionic surface-imprinted polymers was similar, except that no template ion was added, and no elution step was required. The polymer obtained was labeled as La-NIP [11, 12].

2.3 Adsorption Procedure

2.3.1 Static Adsorption Experiment

An appropriate amount of the prepared adsorbent was added to an Erlenmeyer flask containing La^{3+} solutions with different concentrations, then sealed in a constant-temperature shaking box and shaken until adsorption saturation was reached. Then the filtrate was added to a 25 mL volumetric flask containing hydrochloric acid and arsenazo (III) solution and diluted it. Let it stood for a period of time to allow the lanthanum ions to completely complex with azozone (III), then measured the absorbance of the solution. The adsorption amount was calculated from the standard curve using formula (1):

$$Q = \frac{(c_o - c_e) \cdot V}{m} \tag{1}$$

where Q is the adsorption amount of the adsorbent (mg/g), C_0 is the initial concentration of the rare earth ion (mg/L), C_e is the concentration of the lanthanum ion at adsorption saturation (mg/L), V is the volume of the solution (L), and m is the mass (g) of the added adsorbent.

2.3.2 Study on Selective Recognition of Lanthanum Ions

Coexisting solutions containing La^{3+} and Gd^{3+}, Ce^{3+}, Fe^{3+}, Yb^{3+}, or Al^{3+} were created with the same concentrations, and the adsorbent was added and allowed to reach saturated adsorption. The concentration of each ion in the solution was measured by ICP, and each partition coefficient Kd of metal ions was calculated using formula (2). And the selectivity coefficient k and the relative selectivity coefficient k' were calculated according to formulas (3) and (4). The specific recognition ability of the adsorbent was analyzed according to k.

$$K_d = \frac{Q_e}{C_e} \tag{2}$$

$$k = \frac{K_d(La)}{K_d(M)} \tag{3}$$

$$k' = \frac{k_{IIP}}{k_{NIP}} \tag{4}$$

where K_d is the distribution coefficient, k is the selectivity coefficient of La^{3+}, k' is the relative selectivity coefficient of ion-imprinted k_{IIP} and non-imprinted k_{NIP}.

2.4 Characterization Methods

Fourier-transform infrared (FTIR) spectroscopy, transmission electron microscopy (TEM), and scanning electron microscopy (SEM) were used to characterize the adsorbents. The concentration of rare-earth ions in solutions was measured using a spectrophotometer, and the concentration of the mixed ions was measured by ICP.

3 Results and Discussion

3.1 Characterization of Lanthanum Ion-Imprinted Polymers

3.1.1 SEM Analysis

SEM images of imprinted polymer La-IIP and non-imprinted polymer La-NIP are shown in Fig. 1. There is no obvious difference between La-IIP and La-NIP, indicating that modifying the support MCM-41 and subsequent polymerization did not affect the crystal structure of the support, which indicates that MCM-41-2 is stable. The figure also shows that the prepared polymer has good dispersion and no obvious agglomeration [13, 14].

3.1.2 TEM Analysis

Figure 2 shows a TEM image of La-IIP and La-NIP. The pore structure of La-IIP and La-NIP did not significantly change, indicating that the modification to the MCM-41-2 support and subsequent polymerization did not change the crystal form of the support. However, both La-IIP and La-NIP collapsed the channels, and the non-imprinted polymers collapsed more significantly. La-IIP functional monomers

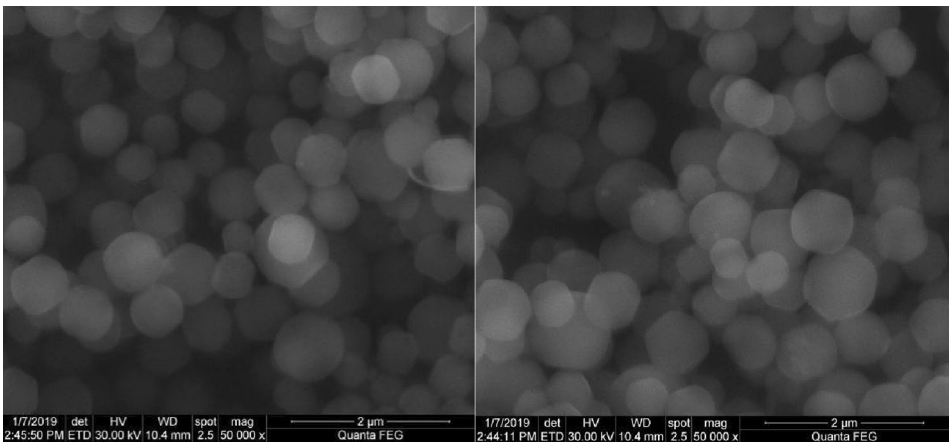

Fig. 1 SEM image of La-IIPand La-NIP

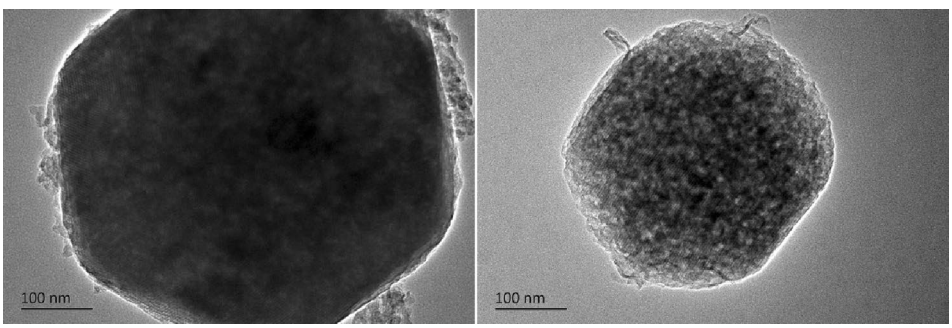

Fig. 2 TEM image of La-IIP and La-NIP

were grafted on the surface of mesoporous materials, interacted with ions, and were protected from subsequent reactions. Finally, they were eluted under acidic conditions to form imprinted holes. Since La-NIP does not interact with ions, the subsequent polymerization reaction was affected, and the collapse of the channels was more obvious [15].

3.1.3 FTIR Analysis

The FTIR spectra of MCM-41-2 and La-IIP in Fig. 3 both contain absorption peaks at 3394 cm^{-1}, 1083 cm^{-1}, 802 cm^{-1}, and 460 cm^{-1}. The peak of La-IIP at 3394 cm^{-1} was significantly broader than that of MCM-41-2 due to interactions between N–H and Si–OH, and also shows that ATPES was supported on MCM-41-2. The peaks at 1083 cm^{-1}, 802 cm^{-1}, and 460 cm^{-1} correspond to asymmetric Si–O–Si stretching, symmetrical stretching, and bending of the molecular sieve, respectively [16, 17]. Compared with MCM-41-2, new absorption peaks appeared at 2943 cm^{-1}, 1458 cm^{-1}, 1382 cm^{-1}, and 1232 cm^{-1} due to La-IIP. The peak at 2943 cm^{-1} was the C–H stretching vibration peak, which was due to the presence of 3-chloropropyltriethoxysilane. The peak at 1232 cm^{-1} corresponded to the C–O–C stretching vibration peak, indicating that epichlorohydrin was crosslinked on MCM-41-2. The peaks at 1458 cm^{-1} and 1382 cm^{-1} corresponded to the CN and CH stretching vibration peaks. The bending vibration peak implies the successful grafting of APTES onto the surface of MCM-41-2 [18].

3.2 Effect of Adsorption Conditions on the Static Adsorption Performance of Adsorbents

3.2.1 Influence of Solution pH on Adsorption

The stock solution was diluted in equal concentrations and transferred to Erlenmeyer flasks. The pH was adjusted to 1, 2, 3, 4, 5, and 6 to investigate the effect of pH on the adsorption properties of lanthanum ion-imprinted polymers and non-imprinted polymers. Figure 4 shows the relationship between the adsorption amount and pH. The adsorption curve trend of adsorption amounts of La-IIP and La-NIP were the same, but La-IIP showed a greater increase than La-NIP, indicating that pH had a greater effect on La-IIP. The adsorption of La-IIP and La-NIP both sharply increased when the pH was increased from 1 to 5, and then began to decrease. The maximum adsorption amounts were 175 mg/g and 125.89 mg/g, respectively. The capacity ion blot was 1.4 times higher than the non-ion blot. The adsorption of lanthanum ions was lower at low pH due to the presence of more free H^+ in the solution which competed with the lanthanum ions and occupied some of the active sites. As the pH increased, the free H^+ decreased, the contact between the lanthanum ions and La-IIP increased, the interaction with amines in APTES increased, and the adsorption capacity increased. The maximum adsorption was reached at pH = 5. When pH > 5, lanthanum ions were hydrolyzed to form hydroxides which reduced the number of free lanthanum ions in the solution, which in turn reduced the amount of adsorption [19, 20].

3.2.2 Adsorption Kinetics

Figure 5 shows the La-IIP and La-NIP adsorption time curves, which shows that La-IIP reached adsorption equilibrium within 10–20 min, while La-NIP reached adsorption equilibrium within 20–30 min. The ion-imprinted polymer

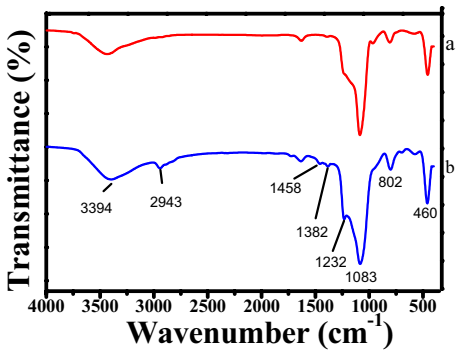

Fig. 3 Infrared spectar of a- MCM-41-2 and b- La-IIP

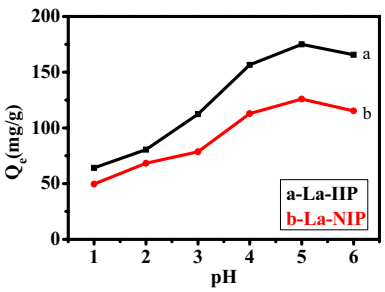

Fig. 4 Influence of pH on La-IIP and La-NIP

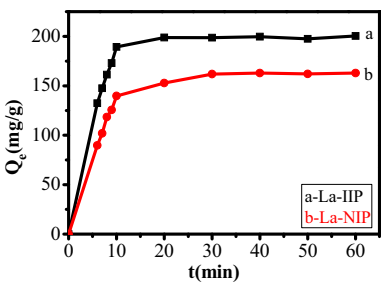

Fig. 5 Time curves of La-IIP and La-NIP

Table 1 The fitting parameters of the quasi-first-order and quasi-second-order kinetic models of La-IIP

Pseudo-first-order equation			Pseudo-second-order equation		
k_1/min	R^2	Q_e/mg/g	$k_2 \times 10^{-3}$/g/(mg min)	R^2	Q_e/mg/g
0.3888	0.9416	619.06	2.9536	0.9986	175.44

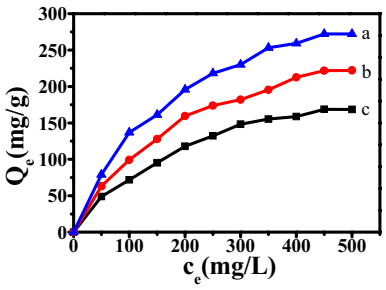

Fig. 6 Influence of initial concentration of solution on La-IIP at different temperatures (a-338 K, b-318 K, c-298 K)

reached adsorption equilibrium faster than the non-ion-imprinted polymer. This was because the ion-imprinted surface contained lanthanum ion vacancies, which more quickly and efficiently adsorbed lanthanum ions from water than non-ion-imprinted polymers, thus shortening the adsorption time. It can also be seen from the figure that the adsorption of La-IIP and La-NIP within 10 min sharply increased, and after 10 min, the adsorption gradually slowed until adsorption equilibrium was reached. However, to ensure that the polymer fully adsorbed lanthanum ions, the adsorption time was set to 1 h [21].

To investigate the adsorption process of lanthanum ions by La-IIP, the adsorption of La-IIP was fitted with quasi-first-order and quasi-second-order kinetic models. The fitting results are shown in Table 1, which shows R^2 values of 0.9936 and 0.9999, respectively. Therefore, it can be concluded that the La-IIP adsorption process followed the quasi-second-order kinetic model. The fitted theoretical maximum adsorption Q_e and the experimentally measured 175.44 mg/g and 168.79 mg/g, respectively. These similar values that La-IIP conformed to a quasi-second-order kinetic model and that the adsorption of the imprinted polymer proceeded mainly via chemical adsorption [22].

3.2.3 Isothermal Adsorption Model

Figure 6 shows the adsorption amounts of La-IIP at 298 K (25 °C), 318 K (45 °C), and 338 K (65 °C). The figure shows that the amount of lanthanum ions adsorbed at different initial concentrations first sharply increased, and then reached equilibrium at about 280 mg/g. The maximum adsorption of 272.2 mg/g was reached at 338 K. The maximum adsorption amounts at 298 K and 318 K were 175.54 mg/g and 222.15 mg/g, respectively. These results show that the adsorption process of La-IIP required energy, so it can be concluded that adsorption proceeded via chemisorption [23, 24].

The adsorption data of La-IIP at 298 K, 318 K, and 338 K were fitted to the Langmuir and Freundlich isotherm models, and the fitting results are shown in Table 2. Comparing the R^2 values shows that La-IIP more closely followed the Langmuir adsorption model, indicating that the adsorption process was monomolecular adsorption. Larger K_L values were obtained at higher temperatures, indicating an endothermic reaction, and that the La-IIP adsorption more closely followed the Langmuir adsorption model [22, 25].

3.2.4 Adsorption Thermodynamics

The values ΔH, ΔS, and ΔG of La-IIP were calculated using Eqs. 5 and 6, and the results are shown in Table 3.

$$\Delta G = \Delta H - \Delta S \cdot T \quad (5)$$

Table 2 Lamuguir and Freundlich adsorption model fitting parameters of La-IIP

Thermodynamic model	Temperature (K)		
	298	318	338
Langmuir			
Equation	y = 0.0046x + 0.6246	y = 0.0035x + 0.4221	y = 0.0032x + 0.2467
R^2	0.9919	0.9941	0.9976
Q_m/mg/g	217.39	285.71	312.5
K_L	0.0074	0.0083	0.013
R_L	0.2636	0.2535	0.182
Freundlich			
Equation	y = 0.5083x + 2.1168	y = 0.4741x + 2.6087	y = 0.4108x + 3.1904
R^2	0.9876	0.9845	0.9665
1/n	0.5083	0.4741	0.4108
K_F	8.3	13.58	24.3

Table 3 Adsorption thermodynamic constants of La-IIP

Adsorption thermodynamic parameters	Temperature (K)		
	298	318	338
La-IIP			
ΔH/kJ/mol		20.71	
ΔS/J/(K mol)		72.54	
ΔG/kJ/mol	−0.91	−2.36	−3.81

$$\mathrm{InK_d} = \frac{\Delta S}{R} - \frac{\Delta H}{RT} \tag{6}$$

It can be seen from the table that $\Delta G < 0$ at 298 K, 318 K, and 338 K, indicating that the reaction was spontaneous. ΔG decreased with increasing temperature, indicating that higher temperatures were more favorable for adsorption [26, 27]. $\Delta H = 20.71$ kJ/mol > 0 kJ/mol, indicating that La-IIP adsorption was an endothermic reaction. Experimental calculations showed that $\Delta G < 0$, $\Delta H > 0$, and $\Delta S > 0$, indicating that adsorption proceeds via an endothermic spontaneous reaction [28, 29].

3.2.5 Selectivity Study

In order to study whether the imprinted La-IIP and the non-imprinted La-NIP could selectively adsorb lanthanum ions, Ce(III), Gd(III), Yb(III), Al(III), and Fe(III) were selected as interfering ions. The corresponding selectivity coefficients were calculated using formulas 2, 3, and 4 to study the selectivity of La-IIP and La-NIP towards lanthanum ions during adsorption. The results are shown in Table 4 [30, 31] and show that the lanthanum selectivity of La-IIP was better than that of La-NIP. The selectivity coefficients for Ce(III), Gd(III), and Yb(III) were 3.63, 5.42, and 3.01, respectively. The selectivity coefficients for Ce(III), Gd(III), and Yb(III) were only 1.16, 1.44, and 1.1. Compared with the reamed MCM-41, La-IIP showed a good selectivity coefficient for La(III). The selectivity coefficients of La-IIP for Al(III) and Fe(III) were 12.32 and 6.7, respectively, indicating that Ce(III), Gd(III), and Yb(III) interfered with La-IIP selectivity and recognition of La(III). Among the relative selectivity coefficients, Al(III) has the highest relative selectivity coefficient of 10.11, indicating that La-IIP could select and recognize La(III).

Table 4 Distribution coefficient and selectivity coefficient of La-IIP and La-NIP

Metal ion	La-IIP		La-NIP		
	K_d (mL/g)	$k_{La/M}$	K_d (mL/g)	$k_{La/M}$	k'
La(III)	631.58		209.94		
Ce(III)	173.91	3.63	197.80	1.16	3.14
Gd(III)	116.40	5.42	116.40	1.44	3.76
Yb(III)	209.94	3.01	197.8	1.10	2.73
Fe(III)	94.24	6.70	285.71	1.00	6.70
Al(III)	51.28	12.32	234.64	1.22	10.11

3.2.6 Elution and Reuse

For imprinted polymers, it is important to consider whether the adsorption of ions after repeated elution affects their selectivity. First, a 2 M HCl solution was selected as the desorption solution, and La-IIP was repeatedly eluted and used to adsorb lanthanum ions. The results show that the adsorption capacity reached more than 81% after five cycles. Similarly, La-IIP was eluted and adsorbed with H_2SO_4, HNO_3, and 0.1 M EDTA. The results showed in Fig. 7 that the desorption capacity of EDTA was the weakest, and HCl was the strongest. After eluting La-IIP with HCl five times, the adsorption remained at its initial value of 81%, indicating the stability and reusability of La-IIP [32].

4 Conclusions

In this paper, surface Lanthanide ion-imprinted polymer La-IIP and non-ionic surface-imprinted polymers La-NIP were prepared with APTES as the functional monomer, reamed MCM-41 as the carrier and epichlorohydrin as the crosslinking agent. The results are summarized as follows:

(1) The La-IIP has strong adsorption affinity, specific recognition ability and excellent selectivity, and the maximum adsorption capacity is 272.2 mg/g.
(2) Through the quasi-first-order and quasi-second-order kinetic fitting of the experimental data, it is concluded that La-IIP is more in line with the quasi-second-order kinetic models, indicated that the adsorption process of La-IIP is mainly chemical adsorption.

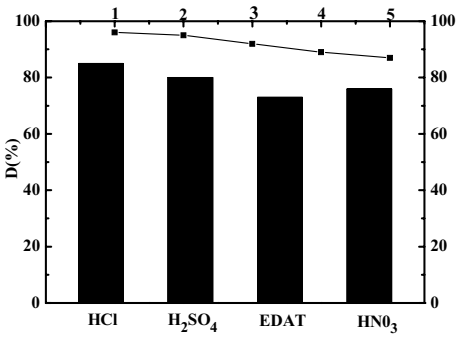

Fig. 7 Desorption efficiency of different elution solvents

(3) According to the isothermal adsorption model, the Langmuir and Freundlich adsorption models of La-IIP were fitted, the results showed that La-IIP was more in line with the Langmuir adsorption model.
(4) The thermodynamic fitting results of La-IIP showed that the adsorption process is an endothermic spontaneous reaction.
(5) In addition, La-IIP has good stability and high availability.

Surface ion imprinting technology continues to develop and become more and more mature, which provides more reference methods for the treatment and adsorption of metal ions in waste ore water. Therefore, this work has a certain reference value for environment-friendly and industry.

Acknowledgements The work was supported by the Nature Science Foundation of China (51664042).

References

1. M.A. Nicodemus, K.F. Salifu, D.F. Jacobs, Influence of lanthanum level and interactions with nitrogen source on early development of *Juglans nigra*. J. Rare Earths **27**(02), 270–279 (2009)
2. S. Zinatloo-Ajabshir, M. Mousavi-Kamazani, Effect of copper on improving the electrochemical storage of hydrogen in CeO_2 nanostructure fabricated by a simple and surfactant-free sonochemical pathway. Ceram. Int. **46**(17), 26548–26556 (2020)
3. S. Zinatloo-Ajabshir, Z. Salehi, O. Amiri, M. Salavati-Niasari, Simple fabrication of $Pr_2Ce_2O_7$ nanostructures via a new and eco-friendly route; a potential electrochemical hydrogen storage material. J. Alloys Compd. **791**, 792–799 (2019)
4. S. Zinatloo-Ajabshir, M.S. Morassaei, O. Amiri, M. Salavati-Niasari, Green synthesis of dysprosium stannate nanoparticles using *Ficus carica* extract as photocatalyst for the degradation of organic pollutants under visible irradiation. Ceram. Int. **46**(5), 6095–6107 (2020)
5. S. Zinatloo-Ajabshir, M. Salavati-Niasari, Photo-catalytic degradation of erythrosine and eriochrome black T dyes using $Nd_2Zr_2O_7$ nanostructures prepared by a modified Pechini approach. Sep. Purif. Technol. **179**, 77–85 (2017)
6. S. Zinatloo-Ajabshir, M. Salavati-Niasari, Preparation and characterization of nanocrystalline praseodymium oxide via a simple precipitation approach. J. Mater. Sci.: Mater. Electron. **26**(8), 5812–5821 (2015)
7. M. Monier, A.A. Ibrahim, M. Metwally, D. Badawy, Surfaceion-imprinted amino-functionalized cellulosic cotton fibers for selective extraction of Cu(II) ions. Int. J. Biol. Macromol. **81**, 736–746 (2015)
8. D. Gao, Z. Zhang, M. Wu, C. Xie, G. Guan, D. Wang, A surface functional monomer-directing strategy for highly dense imprinting of TNT at surface of silica nanoparticles. J. Am. Chem. Soc. **129**, 7859–7866 (2007)
9. L. Xiancai, X. Qian, T. Minglei, W. Xiu, Y. Yifeng, Preparation of lanthanum ion imprinted polymer on the surface of MCM-41 modified by aldehyde group and its adsorption and separation of lanthanum ions. Ion Exch. Adsorpt. **34**(02), 105–115 (2018)
10. W. Wang, Y. Li, B. Gao et al., Effective removal of Fe(II) impurity from rare earth solutionusing surface imprinted polymer. Chem. Eng. Res. Des. **91**, 2759–2764 (2013)
11. H. Zhao yong, Preparation of surface ion imprinted polymer based on mesoporous silica material and study on its selective separation for heavy metal ions. Jiangsu Univ. Sci. Technol. (2015)
12. D. Macquarrie, D. Jackson, J.G. Mdoe, J.H. Clark, Organomodifed hexagonal mesoporous silicates. New J. Chem. **23**, 539–544 (1999)
13. H. Dedong, H. Husheng, C. Dingkai et al., Synthesis and application of rare-earth elements (Gd, Sm, and Nd) doped ceria-based solid solutions for methyl mercaptan catalytic decomposition. Catal. Today **281**(3), 559–565 (2017)
14. J. Wang, J. Wei, J. Li et al., Straw-supported ion imprinted polymer sorbent prepared by surface imprinting technique combined with AGET ATRP for selective adsorption of La3+ ions. Chem. Eng. J. **293**, 24–33 (2016)
15. Li. Xiancai, Z. Song, T. Minglei, Preparation and adsorption properties of rhodium ion imprinted polymer Rh-IIP-MAA/MCM-41. J. Nanchang Univ. (Science Edition) **44**(02), 143–147 (2020)
16. M. Li, C. Feng, M. Li et al., Synthesis and application of a surface-grafted In (III) ion-imprinted polymer for selective separation and pre-concentration of indium (III) ion from aqueous solution. Hydrometallurgy (2015). https://doi.org/10.1016/j.hydromet.2015.03.011
17. X.M. Zheng, R.Y. Fan, Z.K. Xu, Preparation and property evaluation of Pb(II) ion-imprinted composite membranes. Acta Polym. Sin. **05**, 561–570 (2012)
18. X. Song, Y. Zhang, C. Yan et al., The Langmuir monolayer adsorption model of organic matter into effective pores in activated carbon. J. Colloid Interface Sci. **389**(1), 213–219 (2013)
19. Li. Xiancai, Hu. Yue Longlong, Z.S. Quanhong, T. Minglei, Adsorption kinetics and thermodynamics of Rhodium ions on RH-IIP-MAA /MCM-41 imprinted polymer. J. Nanchang Univ. (Engineering Science) **41**(04), 307–311 (2019)
20. J.J. Chen, K.M. Fang, Y.Q. Miao et al., Study on adsorption of Co(II) and Ni(II) onto mesoporous Ti- containing MCM-48. J. Nanosci. Nanotechnol. **11**, 1–8 (2011)
21. Li. Chuangju, *Study on the Adsorption of Functionalized Mesoporous Material MCM-41 toward Copper Ion in the Wastewater* (ChongQi University, Chongqing, 2010)
22. L. Firdaous, B. Fertin, O. Khelissa et al., Adsorptive removal of polyphenols from an alfalfa white proteins concentrate: adsorbent screening, adsorption kinetics and equilibrium study. Sep. Purif. Technol. **178**, 29–39 (2017)
23. C. Rui, *Preparation of Surface Ion-Imprinted Polymer Based on SBA-15 and Study on Its Selective Separation Properties for Low and Medium Radioactive Metal* (Jiangsu University of Science and Technology, Zhenjiang, 2014)
24. M. Akram, H.N. Bhatti, M. Iqbal et al., Biocomposite efficiency for Cr(VI) adsorption: kinetic, equilibrium and thermodynamics studies. J. Environ. Chem. Eng. **5**(1), 400–411 (2017)
25. Z. Ye, D. Chen, Z. Pan et al., An improved Langmuir model for evaluating methane adsorption capacity in shale under various pressures and temperatures. J. Nat. Gas Sci. Eng. **31**, 658–680 (2016)
26. X. Qian, *The Preparation of Antimony Ionic Imprinted Polymers and Theiradsorption Properties for Antimony Ions* (NanChang University, Nanchang, 2018)
27. M.A. Shaker, Adsorption of Co(II), Ni(II) and Cu(II) ions onto chitosan-modified poly(methacrylate) nanoparticles: dynamics, equilibrium and thermodynamics studies. J. Taiwan Inst. Chem. Eng. **57**, 111–122 (2015)
28. L. Xiancai, T. Minglei, C. Yuwen, W. Xiu, Preparation and characterization of lanthanide MCM-41 imprinted polymers. J. Nanchang Univ. (Engineering Science) **40**(4), 307–311 (2018)
29. B. Wang, D. Zhang, Z. Shi, T. Wu, Thermodynamics analysis of cesium adsorption on $Na_2Ti_2O_3SiO_4{\cdot}2H_2O$. J. Isot. **25**(1), 42–46 (2012)

30. Q. Fu, Y. Deng, H. Li et al., Equilib-rium, kinetic and thermodynamic studies on the adsorption of the toxins of *Bacillus thuringiensis*, subsp. kurstaki, by clay minerals. Appl. Surf. Sci. **255**(8), 4551–4557 (2009)
31. B. Gao, Y. Zhang, Y. Xu et al., Study on recognition and separation of rare earth ions at picometre scale by using efficient ion-surface imprinted polymer materials. Hydrometallurgy **150**, 83–91 (2014)
32. Z. Adibmehr, H. Faghihian, Preparation of highly selective magnetic cobalt ion-imprinted polymer based on functionalized SBA-15 for removal Co^{2+} from aqueous solutions. J. Environ. Health Sci. Eng. **17**(2), 1213–1225 (2020)